Insulating Behavior at the Neutrality Point in Single-Layer Graphene

F. Amet, J. R. Williams, K. Watanabe, T. Taniguchi, and D. Goldhaber-Gordon

Phys. Rev. Lett. **110**, 216601 — Published 22 May 2013

DOI: 10.1103/PhysRevLett.110.216601

Insulating behavior at the neutrality point in single-layer graphene

F. Amet,[1] J. R. Williams,[2] K.Watanabe,[3] T.Taniguchi,[3] and D. Goldhaber-Gordon[2]

[1]*Department of Applied Physics, Stanford University, Stanford, CA 94305, USA*
[2]*Department of Physics, Stanford University, Stanford, CA 94305, USA*
[3]*Advanced Materials Laboratory, National Institute for Materials Science, 1-1 Namiki, Tsukuba, 305-0044, Japan*

The fate of the low-temperature conductance at the charge-neutrality (Dirac) point in a single sheet of graphene is investigated down to 20 mK. As the temperature is lowered, the peak resistivity diverges with a power-law behavior and becomes as high as several Megohms per square at the lowest temperature, in contrast with the commonly observed saturation of the conductivity. As a perpendicular magnetic field is applied, our device remains insulating and directly transitions to the broken-valley-symmetry, ν=0 quantum Hall state, indicating that the insulating behavior we observe at zero magnetic field is a result of broken valley symmetry. Finally we discuss the possible origins of this effect.

The ability to create electronic devices in graphene has made it possible to study 2D Dirac fermions in the solid state [1]. Transport measurements in a large magnetic field display quantum Hall plateaus with unconventional values of conductance, a signature of the Dirac equation describing electrons in graphene [1, 2]. When the cyclotron gap becomes larger than disorder-induced fluctuations in the surrounding potential, the effect of the linear Dirac band structure becomes evident. At zero magnetic field, the disorder landscape dominates [3], blurring the interesting phenomena that might occur at the Dirac point. Recently, the influence of disorder has been reduced by either suspending a sheet [4] or placing it on atomically-flat boron nitride (BN) [5], and many discoveries in transport have been made due to the more readily-accessible Dirac point in these cleaner system [6–8]. Anomalous patterns in the magneto-conductance attributed to the Hofstadter spectrum were seen to arise when the BN lattice is nearly aligned with the graphene lattice [9, 10].

The nature of the conductivity at the charge-neutrality point σ_{CNP} has been debated since the first graphene-based devices were fabricated. Theory for ballistic graphene predicts a value of $4e^2/\pi h$ for σ_{CNP} [11–13]. However, early experiments on graphene measured σ_{CNP} from 2 to $12\,e^2/h$ [14, 15]. It was soon realized that σ_{CNP} was sample-dependent, determined by the density of carriers in electron and hole puddles produced by static charges on or near the sheet of graphene [16]. In suspended graphene devices [4] the conductivity showed a more pronounced temperature dependence, but still saturated at low temperature and remained higher than $4e^2/\pi h$. Recently the potential landscape in graphene has been made artificially clean by screening potential fluctuations with a second nearby, doped graphene sheet [17, 18]. In that work, instead of saturating at values near e^2/h, σ_{CNP} dropped with a power-law temperature dependence T^α, where α=2 for the most insulating samples, down to T=4 K. Further, the authors observed a strong magnetoresistance in the temperature regime above 10 K and attributed it to weak localization, inferring that ultra-clean graphene may be an Anderson insulator. Alternatively, it has been postulated [19] that this temperature dependence reflects increasing order causing the sample to become more insulating at low density. Here $\sigma_{CNP} \propto T^\alpha$ naturally emerges as the temperature dependence of conduction through a landscape of electron and hole puddles. A complete understanding of this insulating behavior, so far appearing only in graphene on BN, is lacking.

In this Letter, we report on electronic transport in thirteen single-layer graphene devices, some with a top gate and some without. For the two devices where the topgate is the closest to the graphene (∼70 nm), the conductivity at the charge neutrality point (CNP) decreases by more than 2 orders of magnitude with decreasing temperature, whereas the non top-gated samples show a more conventional temperature dependence. Here we focus on one top-gated device where the dependence of the conductance at the CNP (g_{CNP}) on temperature (T) and perpendicular magnetic field (B) is investigated at temperatures down to 20 mK. The temperature dependence is very strong down to T=400 mK and can be fit to a power-law $g_{CNP} \propto T^\alpha$ with $\alpha \approx 0.48 \pm 0.05$. Application of B drives the system more insulating, where at B∼100 mT the ν=0 state is entered, with no intermediate transition to the $2\,e^2/h$ quantum Hall plateau, indicating that a spin or valley (or both) symmetry is broken at very low fields. This direct transition to the ν=0 state has not been observed before in graphene. We speculate on the origin of this effect.

We fabricated our devices using hexagonal-boron nitride (h-BN) as a substrate for graphene, with good electronic properties [5, 20] resulting from the flatness and cleanliness of h-BN flakes. Details of the fabrication are described in Ref. [21] and a schematic of the top-gated device geometry is shown in Fig. 1(a). Our devices are 3 μm long and 1 μm wide, with a top-gate above the middle third of the device. Graphene devices were measured in two different cryostats: a variable-temperature insert enabling temperature-dependent transport measurements from 300 K down to 1.7 K, and a dilution fridge where

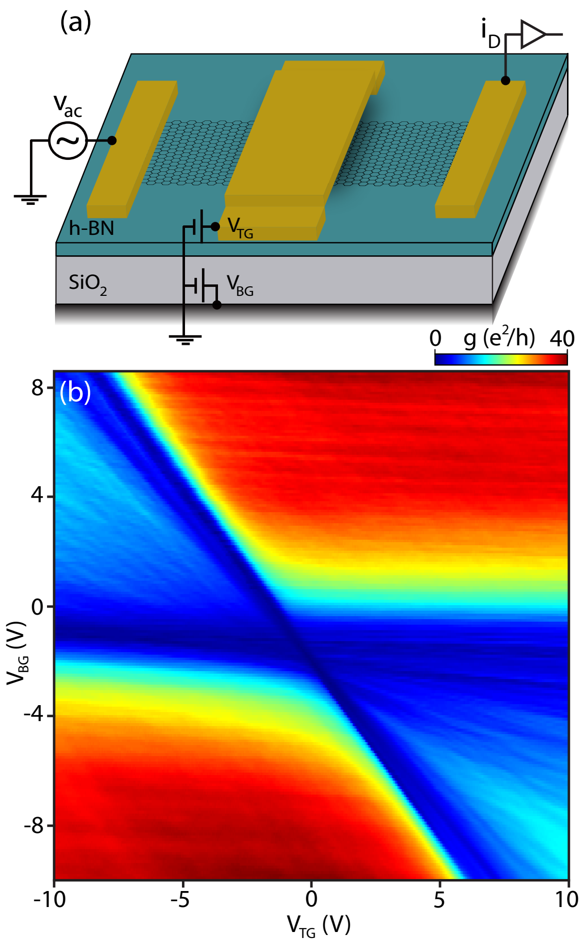

FIG. 1: (a) Schematic of the device in voltage biased mode. A bias v_{AC} is applied to the sample, current i_D is collected at the drain and measured with a lock-in amplifier. A voltage V_{BG} is applied to the degenerately-doped substrate to control the carrier density in the whole sheet. V_{TG} is applied to a suspended metallic gate, 70 nm above the graphene sheet, which varies the carrier density underneath it. (b) Conductance g as a function of both gate voltages, measured at a temperature T=4 K.

samples were measured at lower temperatures, down to 20 mK. We sometimes observed small shifts ($\leq$1V) in the Dirac point position between cool-downs, but no noticeable change in mobility or peak resistance. The conductance g is determined in a standard voltage-biased lock-in measurement with an excitation voltage of 4 μV at 92.3Hz. The resistance r is defined as $1/g$. DC voltages are applied to the top-gate (V_{TG}) and back-gate (V_{BG}). A table of all thirteen devices measured in this work, including mobility and resistance at the CNP ($r_{CNP} = 1/g_{CNP}$) can be found in Ref. [21].

g is shown in Figure 1(b) as a function of V_{TG} and V_{BG} at T=4 K. The carrier density can be controlled independently and with either polarity underneath and outside the top-gated region. As in previous work on dual-gated graphene [22, 23], g exhibits local minima along two intersecting lines corresponding to each region being tuned through the CNP. However, unlike in typical dual-gated graphene devices, g_{CNP} is much smaller than e^2/h along these lines. g was also measured in a 4-probe geometry with similar results, ruling out poor contact resistance at the CNP as the source of this result. Underneath the top-gate, $C_{TG}V_{TG} + C_{BG}V_{BG} = 0$ (where C_{TG} is the top gate capacitance and C_{BG} is the back gate capacitance) at the CNP, yielding a top-gate-to-back-gate capacitance ratio of 1.3 from the slope of the diagonal line in the (V_{BG}, V_{TG}) plane. C_{BG} is $5.94(\pm 0.5)\times 10^{10}\text{cm}^{-2}\text{V}^{-1}$, as extracted from the periodicity of Shubnikov-de-Haas oscillations. Using a parallel-plate capacitance model, we estimate that the top gate is 70 nm away from the flake, which was confirmed by atomic force microscopy. The device exhibits little intrinsic doping, with a CNP voltage of -1 V on the back-gate, and a mobility of 70,000 cm^2/Vs, as extracted from a linear fit to $g(V_{BG})$ at the CNP. We note that the mobility of top-gated and non top-gated regions was comparable, which shows that the suspended gate does not degrade the electronic properties of our device.

Unlike typical graphene samples, r as a function of V_{BG} has a strong temperature dependence in our device (Fig. 2). r_{CNP} dramatically increases at low temperature, from 13 kΩ at T=300 K to 400 kΩ at T=2 K [Fig. 2(a)]. By contrast, r_{CNP} for all devices without a top gate is typically around 10 kΩ at 2 K [21], including for a separate device made in the same sheet of graphene as the device shown on Fig. 2 but without a top-gate. This is comparable to what is commonly seen in good-quality, single-layer graphene devices. The top-gated sample has an insulating temperature dependence close to the CNP, for -1.8 V$\leq$ V_{BG} $\leq$0 V, whereas for higher carrier densities it is metallic [inset, Fig. 2(a)]. A slight shoulder appeared on the left-side of the resistance peak in the second of two cool-downs [Fig. 2(a)], which we attribute to a small doping discrepancy between the top-gated and non-top-gated regions, on the scale of 10^{10} cm^{-2}.

r_{CNP} was measured at lower temperature in a separate cool-down using a dilution fridge: further lowering T to 400 mK increases r_{CNP}, at which point it measures 2.3 MΩ [inset, Fig. 2(b)], then remains constant down to 20 mK within experimental error. Fig. 2(b) shows $g_{CNP}(T)$, which follows a power law $g_{CNP} \propto T^{\alpha}$ as a function of the temperature, with α=0.48$\pm$0.05. This insulating behavior is not due to the opening of a hard band gap, which would lead to an exponentially-activated conductivity. The temperature dependence is also slower than the T^2 dependence measured in Ref. [17] (and expected from the Boltzmann equation with electron-electron scattering). A temperature dependence similar to ours was reported in suspended graphene [4], although the overall conductance was several orders of magnitude higher and the device was not top-gated.

The peak resistance depends on densities both under and outside the top-gate, as shown in Fig. 3 at T=4 K.

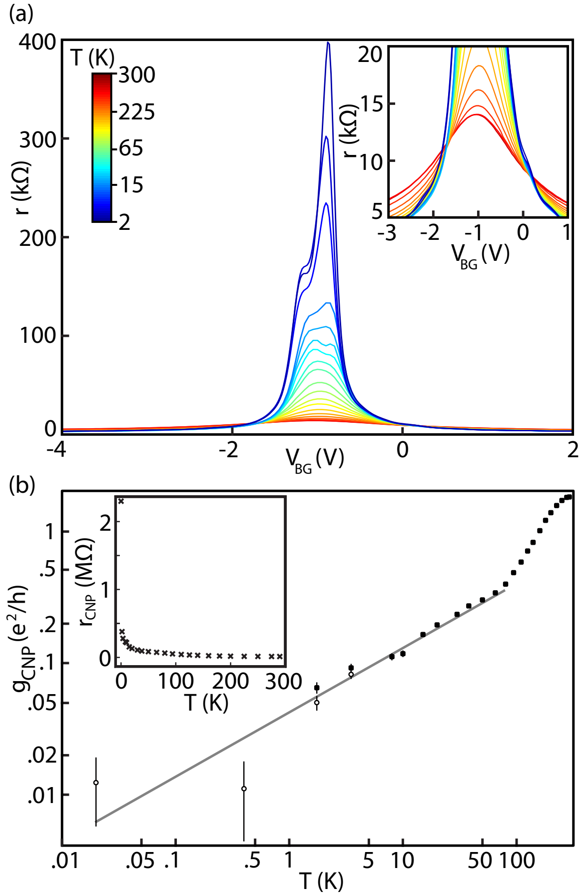

FIG. 2: (a) $r(V_{BG})$ at temperatures ranging from 300 K to 2 K. Inset: close-up view of the intersection of the curves (b) $g_{CNP}(T)$ with open circles and filled squares were measured in the dilution fridge and variable temperature cryostat, respectively. Error bars correspond to one standard deviation: for T>5 K, these are smaller than the dots. The grey line corresponds to a fit $g_{CNP} \propto T^{\alpha}$, with $\alpha = 0.48 \pm 0.05$ for T<80 K. At higher temperature g_{CNP} rises with a faster exponent. Inset: resistance at the neutrality-point r_{CNP} as a function of temperature.

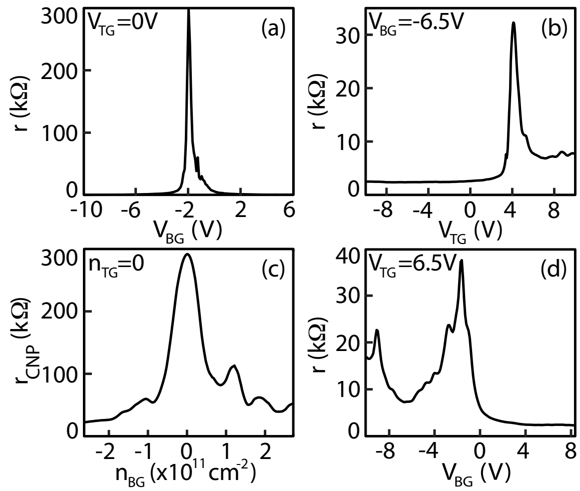

FIG. 3: Cuts of the resistance r measured at T=4K. (a) For a uniform density: r(V_{BG}, V_{TG}=0). (b) As a function of V_{TG}, away from double neutrality: r(V_{TG}, V_{BG}=-6.5V). (c) Keeping the top-gated region at charge neutrality while varying n_{BG}, which is equivalent to varying the perpendicular electric field at fixed n_{TG}: r(n_{BG}, n_{TG}=0). (d) As a function of V_{BG}, away from double-neutrality: r(V_{BG}, V_{TG}=6.5V)

The resistance when the density is uniform - for V_{TG}=0 V - is shown in Fig. 3(a). When the density outside the top-gated region is nonzero [Fig. 3(b)], $r(V_{TG})$ shows the electron-hole asymmetry reported in Ref. [22, 23]. The resistance when the top-gated part of the device is at the neutrality-point (n_{TG}=0) is shown in Fig. 3(c), as a function of the carrier density outside the top-gated region (n_{BG}), which is equivalent to varying the vertical electric field. The device has the largest resistance at double-neutrality ($n_{BG}, n_{TG} \sim 0$), in contrast with bilayer graphene, where a similar plot would produce the largest value of r_{CNP} at large n_{BG}, associated with gap opening by a large transverse electric field [24]. At double charge-neutrality, the two-terminal resistance is dominated by the square top-gated region, so it may be treated as a proxy for resistivity of that region. The local maximum of r(V_{TG},V_{BG}) corresponding to charge-neutrality outside the top-gated region yields r_{CNP} ~32kΩ per square for non-top-gated graphene, which means that the top-gated part of the device accounts for 80% of the 300 kΩ measured at double neutrality.

A low-field fan diagram [$g(V_{BG}, B)$] is measured at T=2 K and shown in Fig. 4(a). Away from the CNP, we observe plateaus for $\nu = 2, 6, 10$ (dashed lines) that are well-developed on the hole side for B>0.5T. The cut g(V_{BG}, B=1 T) shows these plateaus in addition to the ν=0 plateau around the CNP [Fig. 4(c)]. Interestingly, the broken-symmetry ν=0 state seems to persist all the way down to very low fields [dark blue region that runs between V_{BG} ~0 and -1V in Fig. 4(a)]. The minimum conductance g_{CNP} as a function of B is shown in Fig. 4(b). The value of V_{BG} at which the minimum occurs shifts slightly upward with magnetic field, drifting by less than 0.1V as B is increased. $g_{CNP}(B)$ monotonically decreases on a scale of ~100 mT and enters the ν=0 gap without first transitioning to the $2e^2/h$ plateau.

Discussion. The temperature dependence of the peak resistance in graphene is often used to estimate the disorder level in a sample [4]. Cleaner samples show a slightly higher peak resistivity which increases as T is lowered, and saturates when k_BT is smaller than the Fermi energy's fluctuations δE_F. However, this interpretation seems insufficient to explain our data: the temperature dependence in our device is very strong down to $T \approx$ 400 mK which would translate to surprisingly small Fermi energy fluctuations $\delta E_F \approx 40\,\mu eV$ – corresponding to density fluctuations of less than 10^6 cm^{-2} – two orders of magnitude lower than in most reported suspended devices [25].

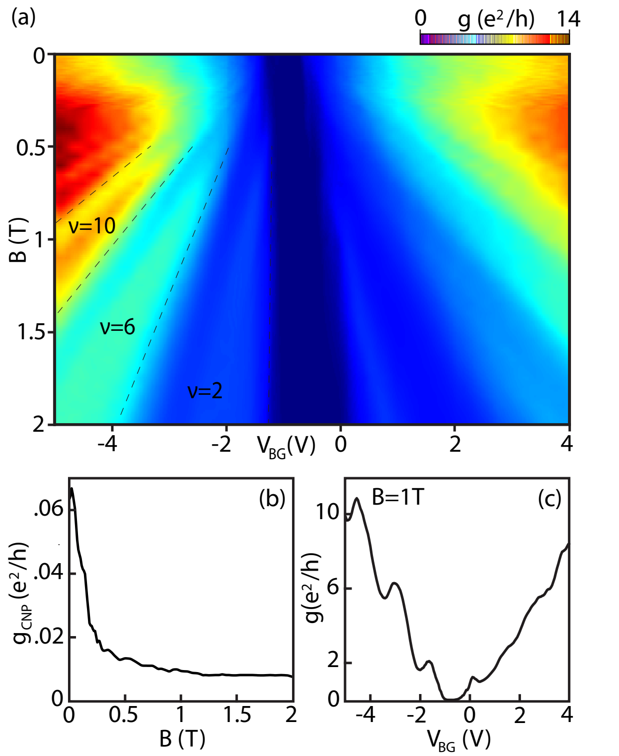

FIG. 4: (a) $g(B, V_{BG})$ measured at T=2 K and in a two-probe configuration. The transitions between plateaus are underlined for ν =0, 2, 6, 10. (b) Minimum conductance as a function of the magnetic field g_{CNP}(B), showing a direct transition to the ν=0 state as a function of B. (c) Cut of g(V_{BG}) at B=1 T.

The presence of a top-gate is likely to contribute to this insulating behavior, since we have yet to observe this effect in non-top-gated devices, and screening by the top-gate could explain reduced density fluctuations. As charge puddles get shallower and further apart, the minimum conductivity is expected to drop as it becomes harder for electrons to percolate [16, 27]. However, the top gate is tens of nanometers away from the flake, significantly further than reported in Ref. [17], and it is therefore surprising that the screening should have such dramatic consequences, as interactions should naively be screened only on distances larger than the spacing to the top gate.

It was recently proposed that in graphene on h-BN devices, electron interactions could enhance the substrate-induced valley-dependent pseudo-potential, hence breaking the valley-symmetry [28–30]. This gap has not been observed yet, but could explain a diverging resistance at the Dirac point in very clean samples. Our low-field magneto-transport data suggest that valley symmetry-breaking may indeed play a role in this insulating behavior. The conductance around the charge neutrality point is never quantized and always very small compared to $2\,e^2/h$ [Fig. 4(b)]. The monotonic decrease of g_{CNP} indicates that the insulating behavior observed at zero field becomes stronger as the magnetic field breaks the valley symmetry and the ν=0 gap opens up. This is qualitatively different from what we and others [21, 32] observed at the CNP for non-top-gated devices: the two-terminal conductance usually develops plateaus at a moderate magnetic field (∼1-2 T). In this regime, g_{CNP} depends on the aspect-ratio of the device [31] but is always on order e^2/h (corresponding to ν=±2). We usually observe that g_{CNP} decreases from $\sim e^2/h$ to zero on a scale of several Tesla, as the valley degeneracy of the n=0 Landau level is lifted [21, 33].

The very steep decrease in the conductance on Fig. 4(b), B=100mT at half-maximum, suggests that either the Landau level broadening is extremely small, or the ν=0 gap grows more rapidly with B than in regular devices. In a magnetic field, the energy of Coulomb interactions is on the order $E_C = \frac{e^2}{\epsilon l_B}$, where l_B is the magnetic length l_B=$\sqrt{\frac{\hbar}{eB}}$. While to first order these interactions preserve valley symmetry, it has been shown that higher-order terms break this symmetry and are on order $\delta E_C = \frac{a}{l_B} E_C$, where a is the spacing between neighboring carbon atoms [32]. A naive estimate of this contribution gives δE_C∼1 meV/T. Interestingly, the field dependence of the ν=0 gap has been studied in Ref [32], where it was found that the effective g factor $g_{\Delta_0} \equiv d\Delta_o/dB$ for the $\nu = 0$ state had this same order of magnitude. Using this result gives a naive upper-bound of $100\mu eV$ for the Landau level broadening due to the Fermi level fluctuations, in good agreement with our previous estimate based on the low-temperature saturation of $g_{CNP}(T)$.

However, the cuts of the resistance shown on Fig. 3 suggest that r under the top-gate doesn't depend solely on n_{TG}. Otherwise, r_{CNP} would only decrease by ∼60 kΩ, the peak resistance of the non-top-gated part of the device, when the two non-top-gated squares of the device are tuned away from charge neutrality, instead of the wide range observed in Fig. 3(c). Due to the roughness of the top-gate, its geometric capacitance is not perfectly uniform, which induces stronger density fluctuations at higher transverse electric field than at double-neutrality. The full width at half-maximum of $r_{CNP}(V_{TG})$ is often used to estimate the disorder level in a sample. At 4K, the width is only δn ∼2.3x10^{10}cm^{-2} at double neutrality but δn ∼1.3x10^{11}cm^{-2} for V_{BG}=-10V. If the insulating behavior we observe is indeed due to the extreme cleanliness of the top-gated part of the device, it is understandable that r_{CNP} decreases at higher gate voltages due to stronger density fluctuations. It is also possible that the interfaces between the top- and non-top-gated regions play a role in the diverging resistance we measured. The resistance of an interface between regions of different densities is not expected to be so high [34], but the interface resistance between two states with different charge correlations might be substantial, and this could come into play if a new state could exist due to screening underneath the top-gate.

We thank A. J. Bestwick, C. R. Dean, P. Gallagher, P. Jarillo-Herrero, M. Y. Lee, L. S. Levitov, J. Sanchez-Yamagishi for useful technical help and fruitful discussions. This work was funded by the Center on Functional Engineered Nano Architectonics (FENA), the W. M. Keck Foundation and the Stanford Center for Probing the Nanoscale, an NSF NSEC, supported under grant No. PHY-0830228. F. Amet acknowledges support from a Stanford Graduate Fellowship.

[1] A. Geim and K. S. Novoselov, Nature Mat. **6**, 183 (2007).
[2] Y. Zhang, Y-W. Tan, H. L. Stormer and P. Kim, Nature **438**, 201 (2005).
[3] J. Martin, N. Akerman, G. Ulbricht, T. Lohmann, J. H. Smet, K. von Klitzing and A. Yacoby, Nature Phys. **4**, 144 (2008).
[4] K. I. Bolotin, K. J. Sikes, J. Hone, H. L. Stormer and P. Kim, Phys. Rev. Lett. **101**, 096802 (2008).
[5] C. R. Dean, A. Young, I. Meric, C. Lee, L. Wang, S. Sorgenfrei, K. Watanabe, T. Taniguchi, P. Kim, K. Shepard and J. Hone, Nature Nano. **5**, 722 (2010).
[6] K. I. Bolotin, F. Ghahari, M. D. Shulman, H. L. Stormer and P. Kim, Nature **462**, 196 (2009).
[7] C. R. Dean, A. F. Young, P. Cadden-Zimansky, L. Wang, H. Ren, K. Watanabe, T. Taniguchi, P. Kim, J. Hone and K. L. Shepard, Nature Phys. **7**, 693 (2011).
[8] D. C. Elias, R. Gorbachev, A. S. Mayorov, S. V. Morozov, A. A. Zhukov, P. Blake, L. A. Ponomarenko, I. V. Grigorieva, K. S. Novoselov, F. Guinea and A. K. Geim, Nature Phys. **7**, 701 (2011).
[9] C. R. Dean, L. Wang, P. Maher, C. Forsythe, F. Ghahari, Y. Gao, J. Katoch, M. Ishigami, P. Moon. M. Koshino, T. Tanaguchi, K. Wantanabe, K. L. Shepard, J. Hone and P. Kim. arXiv:12124783 (2012).
[10] L. A. Ponomarenko, R. V. Gorbachev, D. C. Elias, G. L. Yu, A. S. Mayorov, J. Wallbank, M. Mucha-Kruczynski, A. Patel, B. A. Piot, M. Potemski, I. V. Grigorieva, K. S. Novoselov, F. Guinea, V. I. Fal'ko, A. K. Geim. arXiv:1212.5012 (2012).
[11] J. Nilsson, A. H. Castro Neto, F. Guinea and N. M. R. Peres, Phys. Rev. Lett. **97**, 266801 (2006).
[12] J. Tworzydlo, B. Trauzettel, M. Titov, A. Rycerz and C. W. J. Beenakker, Phys. Rev. Lett. **96**, 246802 (2006).
[13] E. V. Gorbar, V. P. Gusynin, V. A.Miransky, and I. A.Shovkovy, Phys. Rev. B **66**, 045108 (2002).
[14] J. H. Chen, C. Jang, S. Adam, M. S. Fuhrer, E. D. Williams and M. Ishigami, Nature Phys. **4**, 377-381 (2008).
[15] Y.-W. Tan, Y. Zhang, K. Bolotin, Y. Zhao, S. Adam, E. H. Hwang, S. Das Sarma, H. L. Stormer and P. Kim, Phys. Rev. Lett. **99**, 246803 (2007).
[16] S. Adam, E. H. Hwang, V. M. Galitski and S. Das Sarma, PNAS **104**(47), 18392-18397(2007).
[17] L. A. Ponomarenko, A. K. Geim, A. A. Zhukov, R. Jalil, S. V. Morozov, K. S. Novoselov, I. V. Grigorieva, E. H. Hill, V. V. Cheianov, V. I. Fal'ko, K. Watanabe, T. Taniguchi and R. V. Gorbachev, Nature Phys. **7**, 958-961(2011).
[18] K. Kechedzhi, E. H. Hwang, S. Das Sarma, Phys. Rev. B **86**, 165442 (2012)
[19] S. Das Sarma, E. H. Hwang and Q. Li, Phys. Rev. B **85**, 195451 (2012).
[20] J. Xue, J. Sanchez-Yamagishi, D. Bulmash, P. Jacquod, A. Deshpande, K. Watanabe, T. Taniguchi, P. Jarillo-Herrero and B. J. Leroy, Nature Mat. **10**(4), 282-285(2011).
[21] Supplementary information
[22] J. R. Williams, L. DiCarlo and C. M. Marcus, Science **317**, 638 (2007).
[23] B. Huard, J. A. Sulpizio, N. Stander, K. Todd, B. Yang and D. Goldhaber-Gordon, Phys. Rev. Lett. **98**, 236803 (2007).
[24] E. V. Castro, K.S. Novoselov, S. V. Morozov, N. M. R. Peres, J. M. B. Lopes dos Santos, J. Nilsson, F. Guinea, A. K. Geim and A. H. Castro Neto, Phys. Rev. Lett. **99**, 216802 (2007)
[25] A. Mayorov, D. C. Elias, I. S. Mukhin, S. V. Morozov, L. A. Ponomarenko, K. S. Novoselov, A. K. Geim and R. V. Gorbachev, Nano Lett. 12 (9), 4629 (2012).
[26] T. Ando, J. Phys. Soc. Jpn. 75, 074716 (2006).
[27] V. V. Cheianov, V. I. Fal'ko, B. L. Altshuler and I. L. Aleiner, Phys. Rev. Lett. **99**, 176801(2007).
[28] G. Giovannetti, P. A. Khomyakov, G. Brocks, P. J. Kelly and J. van den Brink, Phys. Rev. B **76**, 073103 (2007)
[29] J. C. W. Song, A. V. Shytov and L. S. Levitov, arXiv:1212.6759
[30] M. Kindermann, B. Uchoa and D. L. Miller, Phys. Rev. B **86**, 115415 (2012)
[31] J. R. Williams, D. A. Abanin, L. DiCarlo, L. S. Levitov and C. M. Marcus, Phys. Rev. B **80**, 045408 (2009)
[32] A. F. Young, C. R. Dean, L. Wang, H. Ren, P. Cadden-Zimansky, K. Watanabe, T. Taniguchi, J. Hone, K. L. Shepard and P. Kim, Nature Phys. **8**, 550556 (2012).
[33] Y. Zhang, Z. Jiang, J. P. Small, M. S. Purewal, Y. W. Tan, M. Fazlollahi, J. D. Chudow, J. A. Jaszczak, H. L. Stormer and P. Kim, Phys. Rev. Lett. **96**, 136806 (2006).
[34] V. V. Cheianov, V. I. Falko, Phys. Rev. B **74**, 041403(2006).